

Wirelike Micelle Formed by a T-Shaped Graft Copolymer with a Rigid Backbone

Kwang Hee Kim, June Huh, and Won Ho Jo*

Hyperstructured Organic Materials Research Center and
School of Materials Science and Engineering,
Seoul National University, Seoul 151-742, Korea

Received August 6, 2003

Revised Manuscript Received November 10, 2003

Introduction

Block copolymer in a selective solvent for one of the blocks can form a variety of micellar structures, ranging from spheres, cylinders, or bilayers to more complex bicontinuous structures.^{1–3} These structures can be used in various applications such as drug carriers^{4,5} and nanoporous materials.^{6,7} In such applications, it is necessary to design the molecular structure of block copolymer that would yield a desired micellar structure. Indeed, the molecular architecture is one of the most important molecular factors in determining micellar morphology, since it strongly affects the conformational restriction of block copolymers compatible with the packing geometry of micellar structure. Here, the molecular architecture is determined by a variety of constitutional parameters (e.g., composition, sequence, etc.) and a wide range of topological parameters (e.g., linearity, rigidity, etc.). A number of earlier works have focused on the micellar structures of flexible block copolymers with various architectures and revealed the importance of the composition of hydrophobic block in determining the shape and size of the micelle.^{8–12} In contrast to those extensive investigations on the micellization of flexible block copolymers, relatively few works have been conducted on the effect of chain rigidity on the micellar structure, particularly for nonlinear chain such as graft copolymer.¹³

In this paper, we investigate the micellar structure of amphiphilic T-shaped graft copolymer consisting of a rigid backbone and a flexible side chain in a solvent selective for the flexible side chain by using a Brownian dynamics simulation. In particular, this work focuses on how the conformational restriction of the graft copolymer imposed by both backbone rigidity and chain topology of graft copolymer affects the packing geometry of micellar aggregates.

Model and Simulation

The Brownian dynamics simulations are performed on a cubic box with periodic boundary condition. The chain dynamics is assumed to obey the Brownian dynamics, and hence the equation of motion is given by¹⁴

$$m_i \dot{\mathbf{v}}_i(t) = -m_i \xi_i \mathbf{v}_i(t) + \mathbf{F}_i\{\mathbf{x}_i(t)\} + \mathbf{R}_i(t) \quad (1)$$

where m_i is the mass of particle i , and \mathbf{x}_i , \mathbf{v}_i , \mathbf{F}_i , and ξ_i denote the position, velocity, sum of all forces, and frictional (damping) coefficient acting on the particle i , respectively. In the Brownian dynamics, the effect of solvent molecules is implicitly treated by friction ξ_i and

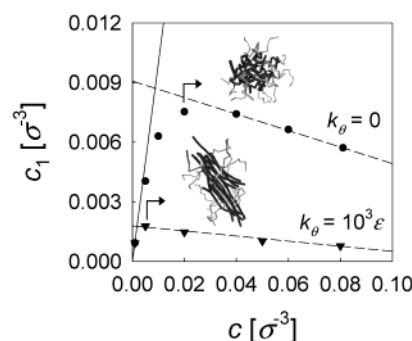


Figure 1. Concentrations of unimers (c_1) as a function of the total chain concentration (c) for T-shaped copolymers of $N_B = 9$ and $N_S = 8$. The solid line indicates the ideal gas behavior ($c_1 = c$), and the dashed lines are linear fits to data points. Snapshots of representative micelles at the concentration slightly above cmc are shown as insets. For clarity, the insoluble backbone chain is represented as thick, dark gray sticks and soluble side chain as thin, light gray sticks.

the random noise term $\mathbf{R}_i(t)$, which is assumed to be stationary and Markovian, to have Gaussian distribution with zero mean and to have neither correlation with prior velocities nor correlation with the systematic forces.

The T-shaped copolymer is modeled by a combination of hydrophobic backbone (B) and hydrophilic side chain (S) grafted at the center of backbone chain. The numbers of beads in the backbone (N_B) and the side chain (N_S) are $N_B = 9$ and $N_S = 4, 8, 16$, and 24 . The harmonic potential is employed for bonded pairs, and the Lennard-Jones (LJ) potential with the well depth ϵ (energy unit) and the bead diameter σ (length unit) is used for nonbonded pairs. Details of the parameter values used for harmonic and LJ potentials are found in our previous publication.¹⁵ To take into account the rigidity of hydrophobic backbone, a bending potential U_θ is introduced by the following formula:¹⁶

$$U_\theta = k_\theta (\cos \theta - \cos \theta_0)^2, \quad \theta_0 = 180^\circ \quad (2)$$

where k_θ is the bending constant and θ is the angle between two successive bonds. The bending constant of a backbone is varied from $k_\theta = 0$ to $k_\theta = 10^3 \epsilon$ while that for flexible side chain remains constant ($k_\theta = 0$). Using a velocity–Verlet algorithm for integration of the equation of motion, the system is equilibrated typically for 1–2 million time steps, after which the structural quantities such as the average aggregation number are changed within statistical error.

Results and Discussion

To determine the critical micelle concentration (cmc), the unimer concentration (c_1) is plotted against the total concentration of T-shaped graft chain (c) for two different cases of $k_\theta = 0$ and $k_\theta = 10^3 \epsilon$, as shown in Figure 1. The cmc is determined from the intersection of the line in the unimer regime ($c_1 = c$) and the second linear line in the micellar regime.¹⁷ The insets in Figure 1 show the snapshot pictures of micellar structures for two cases ($k_\theta = 0$ and $k_\theta = 10^3 \epsilon$) taken at the concentrations slightly above the respective cmc. From the c_1 – c curves in Figure 1, it is observed that the cmcs are $0.0087\sigma^{-3}$ for $k_\theta = 0$ and $0.0018\sigma^{-3}$ for $k_\theta = 10^3 \epsilon$ indicating that

* Corresponding author: e-mail whjpoly@plaza.snu.ac.kr; Tel +82-2-880-7192; Fax +82-2-885-1748.

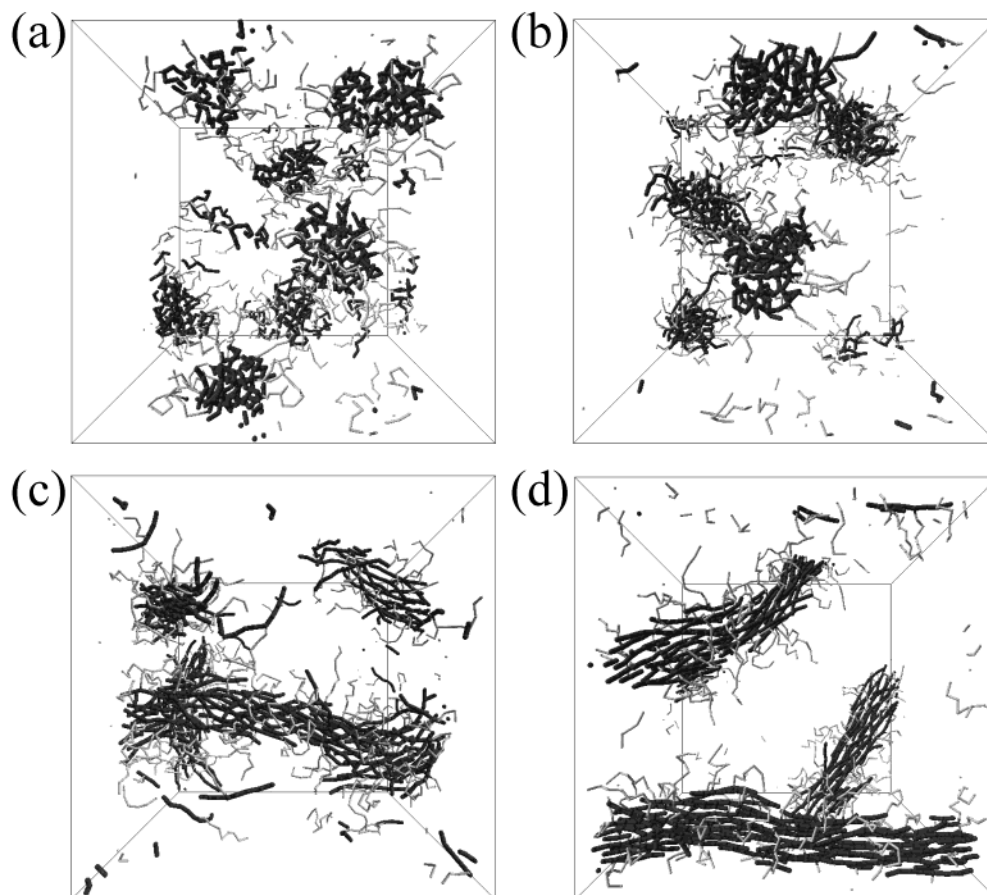


Figure 2. Snapshots of the micellar aggregates formed by T-shaped copolymer ($N_B = 9$ and $N_S = 8$) at different rigidity of backbone chain: (a) $k_\theta = 0$, (b) $k_\theta = 10\epsilon$, (c) $k_\theta = 10^2\epsilon$, and (d) $k_\theta = 10^3\epsilon$. Polymer concentration is fixed as $0.08\sigma^{-3}$ ($n = 144$ in cubic box with the length of one side being 31.1σ). The visual symbols are the same as those in Figure 1.

the micellization of the graft chain with a rigid backbone becomes easier as compared to that with a flexible backbone. This is understandable by the fact that the probability of finding a contact between two neighboring backbones is proportional to the hydrodynamic radius of a backbone chain.

Another interesting feature is that the packing geometry of micellar structure changes from sphere to cylinder as the hydrophobic backbone becomes more rigid. Such morphological change induced by increasing the rigidity of backbone is more clearly illustrated in Figure 2. When the backbone is flexible (Figure 2a), the graft chains form spherical micelles adopting the hair-pinlike conformation of backbone in the core of micelle. As the rigidity of backbone increases, such conformation of backbone chain becomes less favored, and therefore the backbone chain becomes stretched to align with each other, as can be seen in Figure 2.

The cylindrical micelle shown in Figure 2d has unique structural features in two respects. First, the backbones of graft chains in the core of the cylindrical micelle align with each other in such a way that the direction of backbones is perpendicular to the radial direction of cylinder. This molecular packing is strikingly different from the conventional cylindrical micelle^{2,18} formed by flexible diblock copolymers in which the chain direction of hydrophobic block in the core of cylindrical micelle is parallel to the radial direction. When the degrees of alignment of backbones with different bending constants are compared with each other, as listed in Table 1, it is obvious that the chain in the micelles becomes more

Table 1. Degree of Alignment between Backbone Chains in the Micelle

K_θ [ϵ]	f^a
0	0 (0)
10	0.03 (0)
10^2	0.20 (0.01)
10^3	0.53 (0.02)

^a The degree of alignment (f) is determined by the formula $f = \langle \cos^2 \theta \rangle - \langle \cos^2 \theta \rangle_{\text{random}}$ where θ is defined as the angle between two chain vectors with each chain vector being constructed by connecting both ends of backbone of a T-shaped copolymer in the micelle. The value in parentheses denotes the standard deviation.

stretched to the axial direction as the rigidity of backbone chain increases. It is noted that the rodlike micellar structure has been experimentally observed from perfluorosulfonated ionomer (Nafion) in an aqueous solution, in which the fluorocarbon backbone forms the core of the rodlike micelle and the pendant side chain with an ionic group shields the core of the micelle.¹⁹

The second feature of note is that the diameter of core of the micelle is very small such that the length scale of the diameter is an order of bead diameter σ . A measure from Figure 2d reveals that the core diameter is about 3.5σ , which corresponds roughly to 3–4 nm in real scale. Obviously, forming such a thin wirelike micelle is attributed to the fact that the radial growth by the parallel packing of rodlike backbones are limited by the presence of the flexible and hydrophilic side chains connected to the middle point of backbones. To

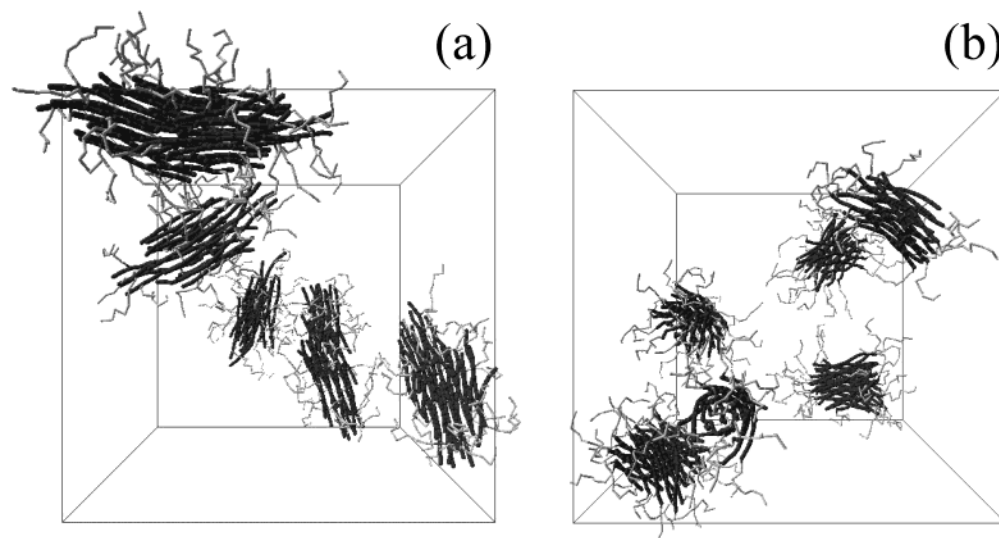


Figure 3. Snapshots of the micellar aggregates formed by T-shaped copolymer ($N_B = 9$ and $N_S = 8$) with side chain grafted onto different positions of polymer backbone: (a) between middle point and end of backbone and (b) at the end of backbone. Polymer concentration is fixed as $0.08\sigma^{-3}$ ($n = 144$ in a cubic box with the length of one side being 31.1σ). The visual symbols are the same as those in Figure 1.

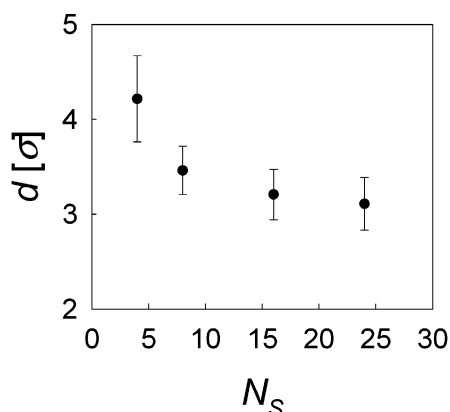


Figure 4. Plot of the diameter of cylindrical micelle vs the length of grafted side chain. The length of insoluble backbone is fixed $N_B = 9$. To keep the concentration of copolymers ($c = 0.08\sigma^{-3}$) unchanged with different chain length, the box size is changed while the number of chain ($n = 144$) is fixed.

examine the size effect of simulation box on the diameter of cylindrical micelle, we simulated micellization by increasing the box size from 31.1σ to 39.2σ in the length of one side and found that the micellar properties (the core diameter and morphology) are nearly unchanged with the size of simulation box.

The grafting position of side chain onto the backbone may also play a crucial role in determining micellar morphology. As the location of junction is changed from the center of rigid backbone to the end of the backbone, the long cylindrical (wirelike) micelle breaks into separate aggregates, as shown in the snapshot pictures of Figure 3, suggesting that the formation of wirelike micelles arises from a combinatorial effect of backbone rigidity and T-shaped architecture.

It is expected that the diameter of a wirelike micelle and its uniformity are dependent upon the length of hydrophilic side chain because the side chain shields the surface of the core in the micelle from exposing to the solvent. When the averaged diameter of the core (d) is plotted against the length of grafted side chain (N_S) at fixed values of $N_B = 9$ and $k_\theta = 10^3\epsilon$, it is realized that the core diameter asymptotically approaches a

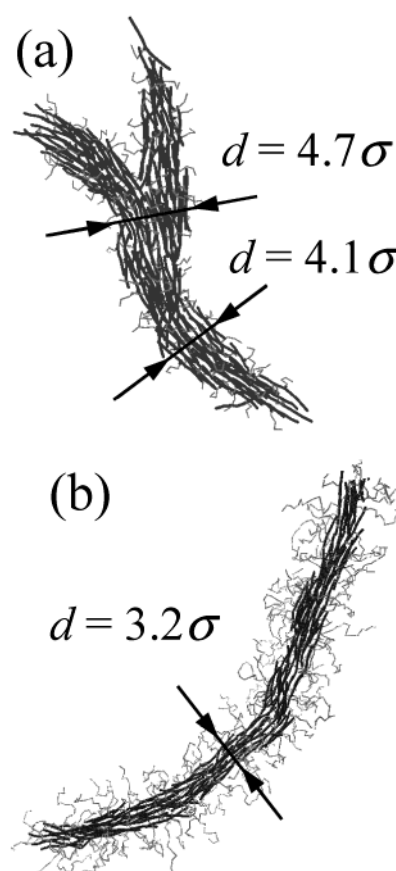


Figure 5. Snapshots of the cylindrical micelle formed by T-shaped copolymer at different length of the soluble block: (a) $N_S = 4$ and (b) $N_S = 16$. The visual symbols are the same as those in Figure 1.

value for the minimal packing in the radial direction as the length of the side chain increases, as shown in Figure 4. It suggests that the core diameter is nearly unchanged if the side chain is sufficiently long. This observation is verified by comparing two representative snapshots of cylindrical micelles formed by the copolymers with short ($N_S = 4$) and long side chain ($N_S = 16$), as shown in parts a and b of Figure 5, respectively. In

summary, as the length of soluble graft chain increases, cylindrical micelle becomes longer in axial direction and more uniform in diameter. Here, it is noted that the branched structure of cylindrical micelle observed for $N_S = 4$ is due to the fact that the length of soluble block is too short to cover the surface of cylindrical core effectively.

Acknowledgment. The authors thank the Korea Science and Engineering Foundation (KOSEF) for financial support through Hyperstructured Organic Materials Research Center (HOMRC). J. Huh thanks the Ministry of Education, the Republic of Korea, for financial support through the BK21 program.

References and Notes

- (1) Hamley, I. W. *The Physics of Block Copolymers*; Oxford University: New York, 1998.
- (2) Zhang, L.; Eisenberg, A. *Science* **1995**, *268*, 1728–1731.
- (3) Förster, S.; Berton, B.; Hentze, H.-P.; Antonietti, M.; Lindner, P. *Macromolecules* **2001**, *34*, 4610–4623.
- (4) Allen, C.; Maysinger, D.; Eisenberg, A. *Colloids Surf. B: Biointerfaces* **1999**, *16*, 3–27.
- (5) Adams, M. L.; Lavasanifar, A.; Kwon, G. S. *J. Pharm. Sci.* **2003**, *92*, 1343–1355.
- (6) Beck, J. S.; Vartuli, J. C.; Roth, W. J.; Leonowicz, M. E.; Kresge, C. T.; Schmitt, K. D.; Chu, C. T.-W.; Olson, D. H.; Sheppard, E. W.; McCullen, S. B.; Higgins, J. B.; Schlenker, J. L. *J. Am. Chem. Soc.* **1992**, *114*, 10834–10843.
- (7) Scott, B. J.; Wirnsberger, G.; Stucky, G. D. *Chem. Mater.* **2001**, *13*, 3140–3150.
- (8) Förster, S.; Zisenis, M.; Wenz, E.; Antonietti, M. *J. Chem. Phys.* **1996**, *104*, 9956–9970.
- (9) Booth, C.; Attwood, D. *Macromol. Rapid Commun.* **2000**, *21*, 501–527.
- (10) Mortensen, K. *J. Phys.: Condens. Matter* **1996**, *8*, A103–A124.
- (11) Pispas, S.; Hadjichristidis, N.; Potemkin, I.; Khokhlov, A. *Macromolecules* **2000**, *33*, 1741–1746.
- (12) Kreig, A.; Lefebvre, A. A.; Hahn, H.; Balsara, N. P.; Qi, S.; Chakraborty, A. K.; Xenidou, M.; Hadjichristidis, N. *J. Chem. Phys.* **2001**, *115*, 6243–6251.
- (13) Adriani, P.; Wang, Y.; Mattice, W. L. *J. Chem. Phys.* **1994**, *100*, 7718–7721.
- (14) Gottberg, F. K.; Smith, K. A.; Hatton, T. A. *J. Chem. Phys.* **1997**, *106*, 9850–9857.
- (15) Kim, K. H.; Huh, J.; Jo, W. H. *J. Chem. Phys.* **2003**, *118*, 8468–8475.
- (16) Maiti, P. K.; Lansac, Y.; Glaser, M. A.; Clark, N. A.; Rouault, Y. *Langmuir* **2002**, *18*, 1908–1918.
- (17) Lísál, M.; Hall, C. K.; Gubbins, K. E.; Panagiotopoulos, A. Z. *Fluid Phase Equilib.* **2002**, *194–197*, 233–247.
- (18) Won, Y.-Y.; Davis, H. T.; Bates, F. S. *Science* **1999**, *283*, 960–963.
- (19) Jiang, S.; Xia, K.-Q.; Xu, G. *Macromolecules* **2001**, *34*, 7783–7788.

MA035139J